Elastic Stability Limits of Polyethylene and *n*-Alkane Crystals from Molecular Simulation

Nhan-Quyen Nguyen, Mark R. McGann, and Daniel J. Lacks*

Department of Chemical Engineering, Tulane University, New Orleans, Louisiana 70118

Received: July 27, 1999; In Final Form: October 5, 1999

Molecular simulations are carried out to determine the elastic stability limits of polyethylene and *n*-alkane crystals under external stresses. For polyethylene, the instability that occurs at the lowest critical stress corresponds to planes of polymer chains perpendicular to the *a*-axis being shifted along the *c*-axis (which is the chain axis); this simulation result concurs with the previous experimental result that (100)[001] crystallographic slip is the dominant plastic deformation mechanism in polyethylene crystals. For *n*-alkane crystals, the stability of the crystal with respect to isotropic tensile stress is greater for *n*-alkanes with even numbers of carbon atoms, due to more favorable packing at the chain ends. This odd−even effect in the elastic stability is related to the well-known odd−even effect in the melting temperatures of *n*-alkane crystals.

I. Introduction

Systems comprised of polyethylene and *n*-alkane crystals have widespread industrial significance. Additionally, *n*-alkane crystals have biological significance in that they serve as models for lipid membranes. The present investigation uses molecular simulations to determine the elastic stability limits of polyethylene and *n*-alkane crystals; i.e., the maximum stress under which an energy minimum corresponding to the crystal structure exists. The consequences of these elastic stability limits are also addressed.

The elasticity limits of polyethylene have significance in regard to materials processing. The large mechanical stresses that occur during materials processing operations lead to inelastic (plastic) deformation of semicrystalline polymer materials.[1] Although plastic deformation occurs in both the amorphous and crystalline parts of the material, the deformation of the crystalline parts dominate at large stresses. For unoriented materials, the plastic deformation in the crystallites will occur first along a "weak link", because the randomly distributed orientations of the crystallites cause any stress applied to the material to act as normal and shear stresses on all faces of the crystallites. This weak link may possibly be related to the elastic stability limits of the crystallite.

The elastic stability limits of *n*-alkane crystals can provide insight in regard to the odd−even chain length effects of the melting temperature of these crystals. It is well-known that the melting temperatures of *n*-alkane crystals increase with chain length N in a zigzag manner, with the N-even alkanes having relatively higher melting temperatures.[2−4] Although the elastic stability limits are not rigorously related to the thermodynamic stability limits (i.e., melting points) of the crystals, previous investigations have shown a correlation between these two stability limits.[5] Experimental and theoretical investigations have attributed the odd−even melting effect to differences in alkane chain packing of the N-even and N-odd alkanes.[2,6,7] By determining the modes by which the *n*-alkane crystals become elastically unstable, the present simulations can provide additional insight regarding the specific interactions that lead to odd−even effects in *n*-alkane crystals.

II. Computational Method

Molecular mechanics simulations are carried out for perfect infinite crystals. All component atoms are explicitly modeled in the simulations, and the SDFF force field of Palmo et al. is used for the potential energy surface.[8] Ewald methods are used to evaluate the Coulombic and dispersion energy sums.[9]

The *n*-alkane crystals exist in several different structures, depending on the number of carbon atoms in the molecule, N, and the temperature. The *n*-alkanes with N odd and $N \geq 11$ crystallize primarily in the orthorhombic *Pbcm* structure, and the *n*-alkanes with N even and $6 \leq N \leq 26$ crystallize primarily in the triclinic $P\bar{1}$ structure.[10−12] In both the *Pbcm* and $P\bar{1}$ structures, the chain axis is exactly or nearly parallel to the *c*-axis of the crystal. The two structures differ in the packing of chains perpendicular to the chain axis, as shown schematically in Figure 1. The *Pbcm* structure is based on a herringbone packing of the chains, whereas the $P\bar{1}$ structure is based on all chains packing with identical orientations. Note that the *Pbcm* structure consists of two layers of molecules per unit cell; the two layers are displaced relative to each other to minimize the steric interactions of adjacent chain ends. In the limit of very long chain length, the *n*-alkane chains become polyethylene. Polyethylene usually crystallizes in an orthorhombic structure analogous to the *Pbcm* structure (we model here an infinite crystal based on the orthorhombic subcell of polyethylene; i.e., chain folding is not addressed).[13] Because the symmetry of the structures may be reduced under stress, our simulations start with these zero-stress structures but do not impose any symmetry: the structures can vary with respect to all atomic positions and the six independent lattice parameters which describe a fully variable unit cell.

The crystal structure is obtained as a function of stress. Initially, the atomic positions within the unit cell and the six independent lattice parameters are varied to minimize the potential energy at zero stress, using a minimization algorithm.[14] The crystal structure is then obtained for an incrementally increasing stress by one of two methods. In the first method, the lattice parameter i is fixed at the desired strain ϵ_i, whereas the atomic positions and remaining lattice parameters are varied to minimize the potential energy E; the stress σ_i is then obtained from the derivative of the energy E with respect to the strain ϵ_i. In the second method, the enthalpy $H = E - V_0 \sum_j \sigma_j \epsilon_j$ is minimized with respect to all lattice parameters and atomic positions for given stresses σ_j (V_0 is the zero stress volume). These two methods give equivalent results for uniaxial stress, and the second method can be applied to more general multiaxial

10.1021/jp992599z CCC: $18.00
Published on Web 11/12/1999

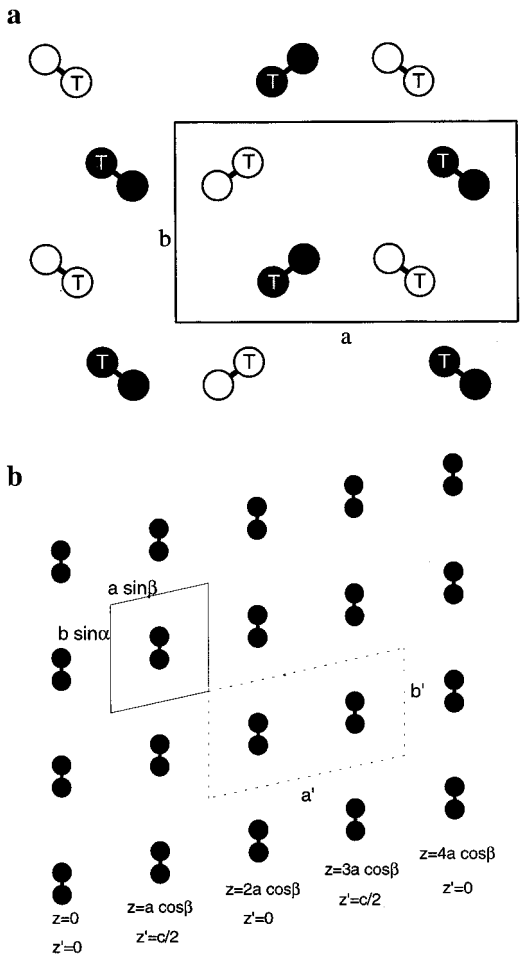

Figure 1. Crystal structures of *n*-alkane and polyethylene systems. (a) Projection along the *c*-axis of the *Pbcm* orthorhombic *n*-alkane structure. The chains are aligned along the *c*-axis, and there are four chains per unit cell (two in an upper layer and two in a lower layer). Filled circles represent chains in the upper layer, open circles represent chains in the lower layer, and the "T" indicates the position of the terminal carbon atoms. The orthorhombic polyethylene structure is given by the filled circles only. (b) Projection along the *c*-axis of the $P\bar{1}$ triclinic *n*-alkane structure. The unit cell is denoted by the solid lines. The chains are tilted with respect to the *c*-axis (not shown), and the neighboring chains along the *a*-axis are shifted along the *c*-axis by the value a cos β, as indicated by the values of *z* at the bottom of the figure.

stresses. Stresses are imposed that correspond to compressive ($\sigma_i < 0$, $i = 1, 2$) and tensile ($\sigma_i > 0$, $i = 1, 2$) stresses perpendicular to the chain axis, and all shear (σ_i, $i = 4, 5, 6$) stresses (compression along the chain axis is not addressed here because it was addressed previously,[15,16] and tension along the *c*-axis is not addressed because instabilities due to this stress in perfect polyethylene crystals involve the breaking of covalent bonds). Simulations are also carried out for isotropic tensile stress ($\sigma_1 = \sigma_2 = \sigma_3 > 0$).

To establish the stability of the crystal structure, possible instability modes of all length scales must be considered. We determine the stability over all length scales by evaluating the normal-mode frequencies in Fourier space,[17] and elastic instabilities are detected by the softening of normal modes (i.e., a normal-mode frequency decreases to zero and becomes imaginary). The softening of a normal mode indicates that the curvature of the potential energy minimum in the direction of the normal mode eigenvector decreases to zero and then becomes negative (in other words, the energy minimum flattens out and then becomes a maximum in this direction). All possible normal modes are accounted for by the wavevectors within the first Brillouin zone.

III. Results

Polyethylene. The stress−strain curves for compression and tension perpendicular to the chain axis are shown in Figure 2. As the crystal is stressed, the magnitude of the strain increases progressively faster until it diverges, after which the crystal structure is no longer stable. Because of strong elastic coupling between the *a* and *b* directions, expansion along one direction leads to compression along the other (and vice versa). The resulting instabilities correspond to changes in the shape of the unit cell; it is the ratio of the lattice parameters that diverges, rather than their product. All unit cells in the crystal change uniformly in this instability, and the analysis of the normal-mode frequencies throughout the Brillouin zone indicate that no elastic instabilities of other length scales precede this divergence of the strain. The values of the critical stresses required to cause these instabilities are given in Table 1.

The stress−strain curve for isotropic tensile stress is shown in Figure 2c. In this case, the divergences of both the *a* and *b* strains are expansive, and the resulting instability is a cohesive failure rather than a change in shape of the unit cell. The critical stress for this instability is significantly greater than that for the shape-change instabilities that arise from uniaxial tension.

The stress−strain curves for shear stresses are shown in Figure 2d. In response to the *bc* and *ac* shear stresses, the elastic instability again comes about through a divergence of the strain with respect to stress (no normal-mode frequencies in the Brillouin zone become imaginary prior to this instability). However, in response to the *ab* shear stress, a normal-mode frequency decreases to zero before the divergence of the strain occurs. The soft mode is a transverse acoustic mode at a finite wavevector in the *ab* plane, which indicates that the instability involves chains moving as rigid units.

The elastic compliance moduli, obtained as the slopes of the stress−strain curves at zero strain, are the following (in inverse gigapascals): $s_{11} = 0.098$, $s_{22} = 0.104$, $s_{12} = -0.053$, $s_{44} = 0.34$, $s_{55} = 0.9$, and $s_{66} = 0.22$. Experimental results are available for only some of these moduli; these experimental values are $s_{11} = 0.15$ GPa^{-1} (for polyethylene at $T = -180$ K)[18] and $s_{44} = 0.5$ GPa^{-1} (for $C_{25}H_{52}$ at room temperature; this value of s_{44} is obtained as the inverse of the value given for the stiffness modulus, which is exactly true for shear moduli of an orthorhombic crystal).[19] The present simulation results for the compliance moduli are in reasonable agreement with experiment. The simulation results underestimate the experimental results because the simulations are at zero temperature, whereas the experiments are at higher temperatures, and thermal effects are known to make the crystal more compliant.

The present simulation method cannot determine the outcome of these instabilities; large-scale simulations must be carried out for this purpose. The outcomes of the instabilities due to uniaxial compression, uniaxial tension, and *ab* shear will likely be phase transitions to other crystalline structures, such as the monoclinic structure that has been detected experimentally in stressed polyethylene samples.[20−22]

***n*-Alkanes.** The changes of the lattice parameters in response to isotropic tensile stress are shown in Figure 3 for the *n*-alkane crystals with $N = 15$ and 16. The elastic instability in response to this stress occurs as a divergence in the expansion along the *c*-axis (the chain axis), for both the *N*-even and *N*-odd alkane crystals (no instabilities at other points in the Brillouin zone occur prior to this divergence). The elastic instability thus occurs

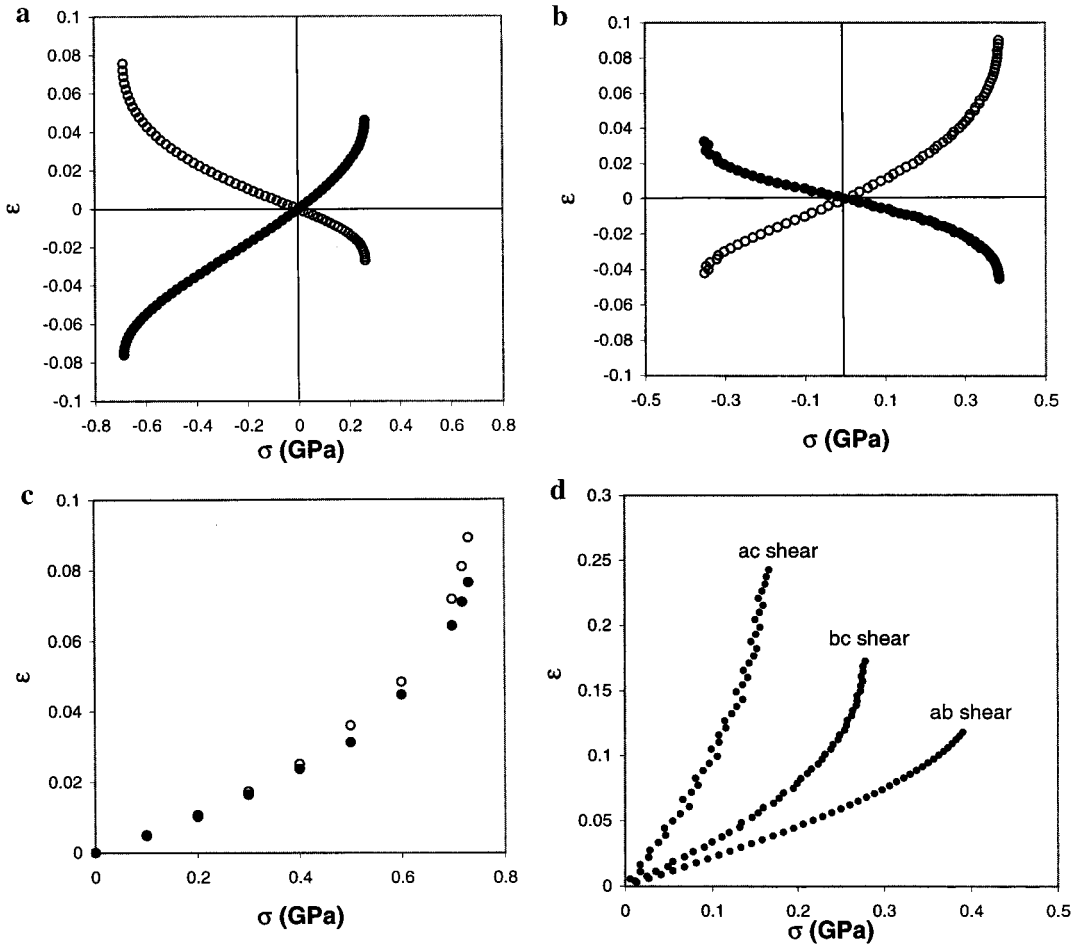

Figure 2. Stress−strain curves for polyethylene. (a) Stress along *a*. (b) Stress along *b*. (c) Isotropic tensile stress. (d) Shear stresses. For parts a−c, closed circles are ϵ_a and open circles are ϵ_b.

TABLE 1: Results for the Elastic Stability Limits of Crystalline Polyethylene

	critical stress (GPa)
compression along *a*	−0.69
compression along *b*	−0.35
tension along *a*	0.26
tension along *b*	0.39
isotropic tension	0.73
ac shear	0.16
bc shear	0.27
ab shear	0.39

by separation of the lamella, and the stability is limited by the interlamellar interactions. Note that the critical stresses for isotropic tensile stress are much smaller for finite-chain *n*-alkanes than for infinite-chain polyethylene, because the instability mechanism of interlamellar separation is not applicable to infinite-chain polyethylene.

The critical stresses in response to isotropic tensile stress for the *n*-alkane crystals are shown as a function of chain length in Figure 4. These results show that the critical stresses are greater for *N*-even alkanes than for *N*-odd alkanes. This difference in elastic stability can be traced to differences in the packing at the interlamellar interface. As shown in Figure 5, each chain end in the *N*-even $P\bar{1}$ crystal has five interlamellar methyl−methyl interactions with separations less than 4.3 Å (the next closest interaction is >4.8 Å). In contrast, each chain end in the *N*-odd *Pbcm* crystal has only three interlamellar methyl−methyl interactions with separations less than 4.3 Å (again, the next closest interaction is >4.8 Å). The greater number of proximate interlamellar methyl−methyl interactions leads to increased cohesive forces in the *N*-even crystals, which necessitates greater stresses to cause an instability.

The linear compressibilities, given by $\chi_i = -(d\epsilon_i/dP)$ evaluated at zero strain, can be determined from the present data (isotropic tensile stress corresponds to negative pressure). The results for the compressibilities for $N = 15$ obtained from the present simulations are $\chi_1 = 0.054$, $\chi_2 = 0.054$, and $\chi_3 = 0.019$ GPa^{-1} (note that these compressibilities are the initial slopes of the curves in Figure 3a divided by the initial values of the corresponding lattice parameters). These simulation results can be compared with the experimental results of Sirota et al.[23] for $N = 21$: $\chi_1 = 0.144$, $\chi_2 = 0.101$, and $\chi_3 = 0.0274$ GPa^{-1}. The simulation results for the compressibility are lower than the experimental results because the simulation results are at zero temperature whereas the experimental results are at higher temperatures. The simulation results agree with those of the experiment in that the compressibility is smallest along the *c* axis.

IV. Discussion

Polyethylene. The randomly distributed orientations of the crystallites within an unoriented semicrystalline material distribute any applied stress as normal and shear stresses on all faces of the crystallites. Plastic deformation thus occurs first at the "weak link" of the crystal, in response to any applied stress. The present results show that the *ac* shear requires the lowest magnitude of stress to cause an elastic instability, as shown in Table 1. The atomic displacements associated with this instability correspond to the (100) crystallographic planes moving in the [001] direction; such displacements define the (100)[001]

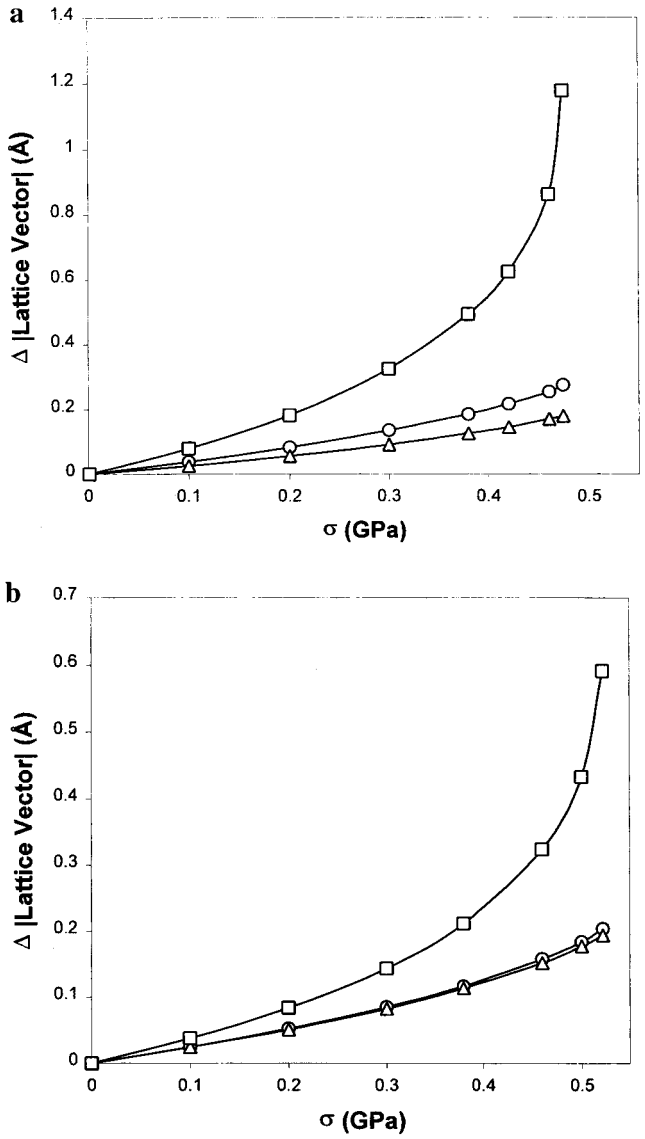

Figure 3. Changes in the magnitudes of the lattice vectors of *n*-alkane crystals in response to isotropic tensile stress. (a) $N = 15$. (b) $N = 16$. The magnitudes of the *a*, *b*, and *c* lattice vectors are represented by circles, triangles, and squares, respectively.

slip system. The simulations thus show that for perfect polyethylene crystals at zero temperature plastic deformation occurs first through elastic instabilities associated with the (100)-[001] slip system.

This simulation result for the primary plastic deformation mode concurs with experiment, which has shown that the dominant mode of plastic deformation in polyethylene crystallites is the (100)[001] slip system.[24−27] However, the simulation result for the critical stress for plastic deformation, 160 MPa, is an order of magnitude larger than the experimental result, ≈10 MPa (this experimental value is the critical resolved shear stress of the (100)[001] slip system).[25,27]

One reason for the difference between the simulation and experimental results is that the simulation results correspond to zero temperature, whereas the experimental results correspond to room temperature. Experimental results are not available for the temperature dependence of the critical stress for the (100)-[001] slip system. However, experimental results show that the critical resolved shear stress for the (010)[001] slip system increases by a factor of 7 over an 85 °C temperature decrease;[28] a similar temperature dependence has been found experimentally

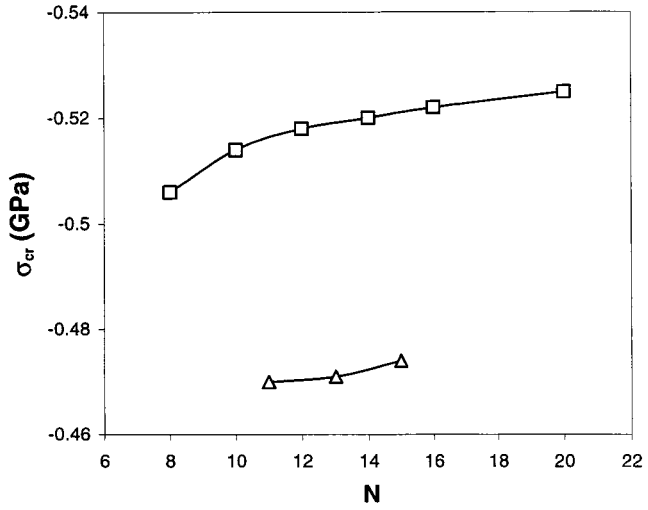

Figure 4. Elastic stability limits of *n*-alkane crystals in response to isotropic tensile stress.

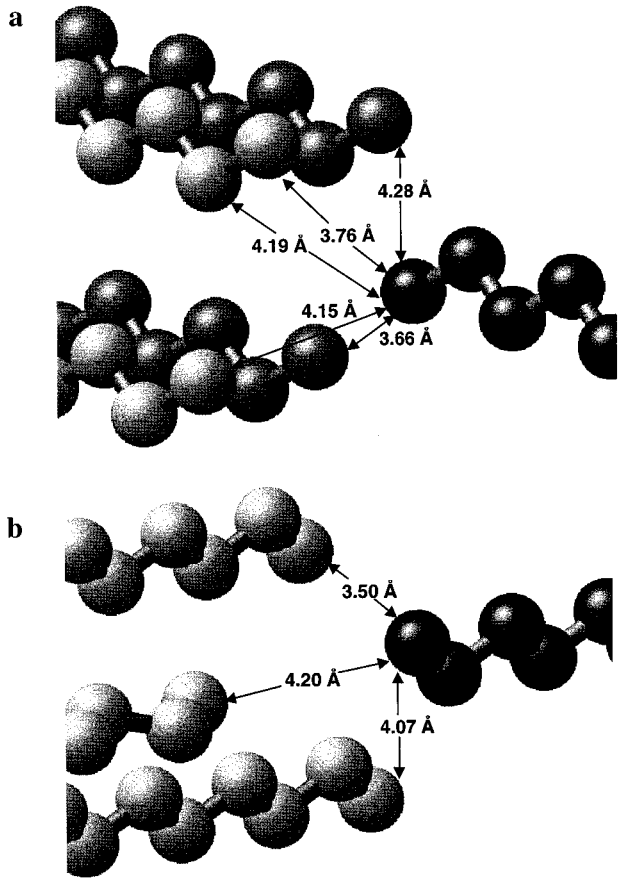

Figure 5. Interlamellar interactions in *n*-alkane crystals. (a) $N = 12$. (b) $N = 13$. All methyl−methyl interactions at separations <4.8 Å are noted.

for nylon crystals.[29] Therefore, for temperatures approaching zero, the experimental value of the critical resolved shear stress of the (100)[001] slip system may very well approach the zero-temperature value obtained in the present simulations.

Another possible reason for the present overestimation of the critical shear stress is that the plastic deformation in real polyethylene crystals can occur through defects (e.g., dislocations) before the elastic stability limits of the perfect crystal are reached. A dislocation mechanism, which has been suggested previously,[25,28,30−32] has yet to be addressed by detailed molecular simulations.

***n*-Alkanes.** The present simulations show that *N*-even crystals have greater stability with respect to isotropic tensile stress than the *N*-odd crystals. This odd−even trend in elastic stability can be related to the odd−even melting effect on the basis of the following approximations:

(1) Tensile stresses mimic the effects of temperature: When the entropy S is expanded about a reference volume, $S(V) = S(V_0) + \sum_i (\partial S/\partial \epsilon_i)\epsilon_i$, the free energy $G = E - \mathrm{TS} - V_0\sum_i \sigma_i\epsilon_i$ can be expressed as $G = E - V_0\sum_i \sigma_i^{eff}\epsilon_i + \mathrm{TS}(T, V_0)$, where the effective stress $\sigma_i^{eff} = \sigma_i + (T/V_0)(\partial S/\partial \epsilon)$. The isotropic tensile stresses used in the present investigation thus mimic the strain dependence of the TS term of the free energy with the approximation that $\partial S/\partial \epsilon_i$ is isotropic.

(2) The elastic instability temperature correlates with the melting temperature. The temperature at which the crystal structure becomes elastically unstable represents an upper-bound to the thermodynamic melting temperature and limits the temperature range of metastability of the superheated crystal.[33,34] Previous investigations have suggested that the instability temperature is correlated with the melting temperature.[5]

On the basis of the above two approximations, the critical stress for elastic stability of *n*-alkane crystals in response to isotropic tensile stress is related to the melting temperature of a crystal, albeit in an approximate way. The advantage of focusing on the critical stress for elastic stability is that the computational intensity of these simulations is relatively small (in comparison to simulations that directly measure the solid−liquid phase equilibrium) and thus high-precision results can easily be obtained even with detailed force fields.

V. Conclusions

The elastic stability limits of polyethylene were determined by molecular simulation. The instability that occurs at the lowest stress corresponds to the (100)[001] slip system. This result concurs with experimental results that show that the (100)[001] slip system is the dominant mechanism for plastic deformation in polyethylene crystals.

The stability of *n*-alkane crystals with respect to isotropic tensile stress exhibits an odd−even chain length effect that is related to the odd−even effect observed experimentally for the melting temperatures. The stability of the *n*-alkane crystals is limited by the interlamellar chain-end interactions; the greater cohesive forces between chain ends in the $P\bar{1}$ *N*-even crystal in comparison to the *Pbcm* *N*-odd crystal gives rise to the odd−even effect.

Acknowledgment. Funding for this project was provided by the National Science Foundation (Grant Number DMR-9624808), the Donors of the Petroleum Research Fund as administered by the American Chemical Society, and the DOE/EPSCoR program.

References and Notes

(1) Lin, L.; Argon, A. S. *J. Mater. Sci.* **1994**, *29*, 294.
(2) Taggart, A. M.; Voogt, F.; Clydesdale, G.; Roberts, K. J. *Langmuir* **1996**, *12*, 5722.
(3) Uhlmann, D. R.; Kritchevsky, G.; Straff, R.; Scherer, G. *J. Chem. Phys.* **1975**, *62*, 4896.
(4) Sirota, E. B.; Singer, D. M. *J. Chem. Phys.* **1994**, *101*, 10873.
(5) Boyer, L. L. *Phys. Rev. Lett.* ***1979***, *42*, 584. Boyer, L. L. *Phys. Rev. Lett.* **1980**, *45*, 1858.
(6) Boese, R.; Weiss, H. C.; Bläser, D. *Angew. Chem., Int. Ed. Engl.* **1999**, *38*, 988.
(7) Malanoski, A. P.; Monson, P. A. *J. Chem. Phys.* **1999**, *110*, 664.
(8) Palmo, K.; Mirkin, N. G.; Krimm, S. *J. Phys. Chem. A* **1998**, *102*, 6448.
(9) Karasawa, N.; Goddard, W. A. *J. Phys. Chem.* **1989**, *93*, 7320.
(10) Norman, N.; Mathisen, H. *Acta Chem. Scand.* **1972**, *26*, 3913.
(11) Craig, S. R.; Hastie, G. P.; Roberts, K. J.; Sherwood, J. N. *J. Mater. Chem.* **1994**, *4*, 977.
(12) Espeau, P.; Robles, L.; Mondieig, D.; Haget, Y.; Cuevas-Diarte, M. A.; Oonk, H. A. J. *J. Chim. Phys.* **1996**, *93*, 1217.
(13) Avitabile, G.; Napolitano, R.; Pirozzi, B.; Rouse, K. D.; Thomas, H. W.; Wills, B. T. M. *J. Polym. Sci., Polym. Lett. Ed.* **1975**, *13*, 351.
(14) Press, W. H.; Teukolsky, S. A.; Vetterling, W. T.; Flannery, B. P. *Numerical Recipes in Fortran: The Art of Scientific Computing*; Cambridge University Press: New York, 1992.
(15) McGann, M. R.; Lacks, D. J. *Phys. Rev. Lett.* **1999**, *82*, 952.
(16) McGann, M. R.; Lacks, D. J. *Macromolecules* **1998**, *31*, 6356.
(17) Ashcroft, N. W.; Mermin, N. D. *Solid State Physics*; Saunders College Press: Philadelphia, 1976.
(18) Buckley, C. P. *J. Mater. Sci.* **1974**, *9*, 100.
(19) Kruger, J. K.; Jimenez, R.; Bohn, K.-P.; Fischer, C. *Phys. Rev. B* **1997**, *56*, 8683.
(20) Frank, F. C.; Keller, A.; O'Conner, A. *Philos. Mag.* **1958**, *8*, 64.
(21) Kiho, H.; Peterlin, A.; Geil, P. H. *J. Appl. Phys.* **1964**, *35*, 1599.
(22) Seto, T.; Hara, T.; Tanaka, K. *Jpn. J. Appl. Phys.* **1968**, *7*, 31.
(23) Sirota, E. B.; Singer, D. M.; King, H. E., Jr. *J. Chem. Phys.* ***1994***, *100*, 1542.
(24) Young, R. J.; Bowden, P. B.; Ritchie, J. M.; Rider, J. G. *J. Mater. Sci.* **1973**, *8*, 23.
(25) Bowden, P. B.; Young, R. J. *J. Mater. Sci.* **1974**, *9*, 2034.
(26) Bartczak, Z.; Cohen, R. E.; Argon, A. S. *Macromolecules* **1992**, *25*, 4692.
(27) Bartczak, Z.; Cohen, R. E.; Argon, A. S. *Macromolecules* **1992**, *25*, 5036.
(28) Young, R. J. *Philos. Mag.* **1974**, *30*, 85.
(29) Lin, L.; Argon, A. S. *Macromolecules* **1994**, *27*, 6903.
(30) Gleiter, H.; Argon, A. S. *Philos. Mag.* **1971**, *24*, 71.
(31) Peterson, J. M. *J. App. Phys.* **1966**, *37*, 4047; *J. App. Phys.* **1968**, *39*, 4920.
(32) Shadrake, L. G.; Guiu, F. *Philos. Mag.* **1976**, *34*, 565; *Philos. Mag.* **1979**, *39*, 785.
(33) Wang, J.; Li, J.; Yip, S.; Wolf, D.; Phillpot, S. *Physica A* **1997**, *240*, 396.
(34) Phillpot, S. R.; Lutsko, J. F.; Wolf, D.; Yip, S. *Phys. Rev. B.* **1989**, *40*, 2831. Lutsko, J. F.; Wolf, D.; Phillpot, S. R.; Yip, S. *Phys. Rev. B* **1989**, *40*, 2841.